Inelastic pion scattering to low-lying excited states of ^{44}Ca

S. Mordechai
Ben-Gurion University of the Negev, Beer-Sheva 84105, Israel
and University of Texas at Austin, Austin, Texas 78712

C. Harvey,* W. B. Cottingame,† P. A. Seidl,‡ and C. Fred Moore
University of Texas at Austin, Austin, Texas 78712

L. C. Bland,§ M. Carchidi, and H. T. Fortune
University of Pennsylvania, Philadelphia, Pennslyvania 19104

S. J. Seestrom-Morris
University of Minnesota, Minneapolis, Minnesota 55455
and Los Alamos National Laboratory, Los Alamos, New Mexico 87545

C. L. Morris
Los Alamos National Laboratory, Los Alamos, New Mexico 87545
(Received 19 December 1986)

Differential cross sections were measured for pion inelastic scattering from ^{44}Ca at $T_\pi = 180$ MeV. The low-lying collective states were analyzed using distorted-wave impulse-approximation calculations with transition densities obtained from electron and previous pion scattering. The cross sections for π^- and π^+ scattering to the low-lying collective states are nearly equal. Neutron and proton matrix elements have been extracted from simultaneous fits to π^- and π^+ data. The resulting values are in good agreement with data from hadronic and electromagnetic probes.

In a previous study of pion inelastic scattering on calcium isotopes[1,2] the low-lying states 0_2^+, 4_1^+, and 2_2^+ in ^{44}Ca were not resolved because of the poor energy resolution of about 300 keV full width at half maximum (FWHM) achieved in that experiment. We have remeasured the pion inelastic scattering on ^{44}Ca, with emphasis on getting an improved energy resolution that would allow us to resolve the triplet at 1.88 MeV (0_2^+), 2.28 MeV (4_1^+), and 2.66 MeV (2_2^+) and to compare experiment with theory for these low-lying states. Our special interest was to look for two-step pion scattering contributions in the 0_2^+ state as well as in other weak low-lying states in ^{44}Ca.

In ^{44}Ca, low-lying 0^+ states have one $(fp)^4$ component and two core-excited pieces—(6p-2h) and (8p-4h).[3,4] The low-lying 2^+ states have two or more $(fp)^4$ terms plus two core-excited pieces in their wave functions.[4] Electromagnetic data give a large $B(E2)$ strength for the γ decay of the first excited 2^+ state to the ground state indicating a strong collective component in the transition. Previous studies have shown that in the energy region of the $\Delta_{3/2,3/2}$ resonance, collective states are strongly excited in pion inelastic scattering.[1,2,5–8] These transitions generally have nearly equal proton and neutron multipole-matrix elements for nuclei with $N \simeq Z$, and therefore have about equal π^+ and π^- inelastic cross sections. Pure neutron or proton excitations have a unique signature in pion scattering that is very different from that for collective transitions.[9] Large π^+/π^- cross-section ratios have already been observed in pion scattering on p-shell nuclei for transitions involving pure proton or pure neutron excitation.[10–12]

Data were obtained using the Energetic Pion Channel and Spectrometer (EPICS) at the Los Alamos Clinton P. Anderson Meson Physics Facility. Cross sections were measured for π^+ and π^- at an incident pion kinetic energy of 180 MeV for scattering angles between $\theta_{\rm lab} = 13°$ and 40°. The strip target consisted of 100-mg/cm^2 metallic calcium enriched to 95.35% in ^{44}Ca and subtended about one-third of the EPICS verticle beam size. The data were taken with reduced flux at forward angles, in order to reduce the counting rates and muon backgrounds. The smallest beam flux was used for π^+ at spectrometer angles of 13° and 19°; an intermediate flux at 25°; and the large flux at angles larger than 25°. For π^- the large flux was used at all scattering angles. Relative normalization of different channel collimator settings was accomplished using an ionization chamber placed in the scattering chamber at 0°, downstream from the target. Muon events in the spectrometer were rejected using a veto scintillator after a graphite absorber.[13] The graphite served to stop the pions while the muons passed through to the veto scintillator. This veto signal was read into the computer and used as a software veto. In addition, at the three most forward angles (13°, 16°, and 19°) we used a hardware veto to reject 99 out of every 100 elastic-scattering events from the hardware trigger. The intent was to lower computer dead time and utilize fewer magnetic tapes for data storage. The data were taken with the total angular acceptance of

EPICS which gives 70% of the events inside of 3° (with a full width of about 5°). The energy resolution obtained was about 150 keV FWHM.

Absolute cross sections were obtained by measuring π^+-p and π^--p yields using a 145.2-mg/cm^2 CH_2 target and by normalizing them to π-p cross sections calculated using the phase shifts of Rowe, Salomon, and Landau.[14] The overall uncertainty in the absolute cross section was estimated to be $\pm 10\%$, and the relative normalization between π^+ and π^- was estimated to be better than $\pm 3\%$.

A typical energy spectrum obtained at a laboratory angle of 34° is presented in Fig. 1. The resolved low-lying 0_2^+, 4_1^+, and 2_2^+ states at 1.88, 2.28, and 2.66 MeV, respectively, are indicated. As can easily be seen from the figure these transitions are extremely weak. For example, the 2_2^+ state at 2.66 MeV is less than one-tenth as strong as the transition to the 2_1^+ state at 1.16 MeV. The same behavior exists in the π^- spectra. The 5% ^{40}Ca in the target presents no background problem in the excitation energy region of interest here, because the 0^+ state at 3.35 MeV is weak[2] and the first 3^- level is at 3.74 MeV. The lines are fits to the spectra obtained using as a reference peak shape the strong transition to the 3^- state at 3.31 MeV in ^{44}Ca with the code FIT.[15] The relative separations between peaks were constrained at values obtained from the energy level compilation.[16] This technique allows reliable extraction of cross sections for the above weak transitions at all angles where they are observed. For the 0^+ state at 1.88 MeV, uncertainties are dominated by the background subtraction. The hardware veto to reject the elastic events mentioned earlier is not a sharp cut in energy and therefore may affect low-lying states. Analysis of the fast clear histograms which include 1% of the rejected events show that the 1.16 MeV state is the only excited state affected by this hardware cut. The multiplicative correction factor for this 2^+ state is estimated to be 1.41 ± 0.11. The correction factor is found to be the same for π^+ and π^-, and is the same at angles of 13°, 16°, and 19°. The cross section reported later in this work for the 2_1^+ state at 1.16 MeV includes the above factor at those forward angles for which the elastic fast clear was used.

Calculations were performed using a modified version of the computer code DWPI,[17] which ties DWPI to the MINUIT optimizer[18] routine. The Kisslinger[19] form of the optical-model potential was used, with parameters obtained from pion-nucleon phase shifts evaluated at an energy 25 MeV below the center-of-mass energy in the pion-nucleus system.[2,20] The collective model was used to obtain the radial shape of the transition density, with different proton and neutron deformation parameters (β_p and β_n, respectively). These parameters were simultaneously varied to reproduce the experimental π^+ and π^- cross sections. The resulting transition densities were integrated to obtain the multipole matrix elements,

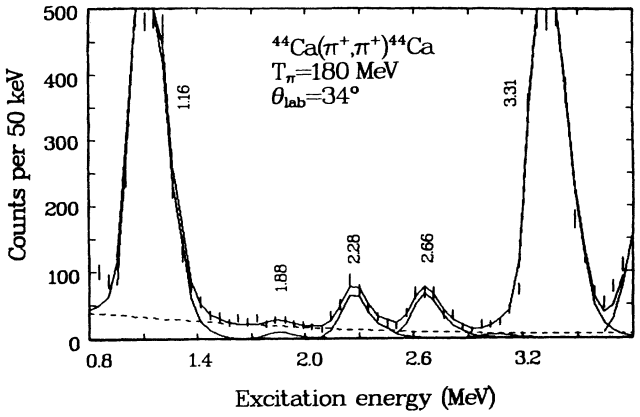

FIG. 1. Missing-mass spectrum and fit for 180-MeV pion scattering from ^{44}Ca at 34° laboratory angle.

$$M_i \equiv e \int_0^\infty r^{l+2} \rho_{\mathrm{tr},i}(r) dr \quad (i = \mathrm{p,n}) \tag{1}$$

with

$$\rho_{\mathrm{tr},i}(r) = -\beta_i R_i \frac{d\rho_i(r)}{dr} \quad \text{for } l \neq 0 , \tag{2}$$

where l is the multipolarity of the transition, $\rho_{\mathrm{tr},i}$ is the proton or neutron transition density, and R_i is the half-density radius. The proton or neutron ground-state density, ρ_i, is parametrized with a three-parameter Fermi distribution,

$$\rho_i(r) = \frac{\rho_0 \left[1 + \dfrac{W_i r^2}{R_i^2} \right]}{1 + e^{[(r - R_i)/a_i]}} \quad (i = \mathrm{p,n}) . \tag{3}$$

We used the same parameters previously determined by Boyer *et al.*[2] from fitting pion elastic scattering data on calcium isotopes at 180 MeV. These are $R_p = 3.75$ fm, $a_p = 0.53$ fm, $R_n = 4.06$ fm, $a_n = 0.47$ fm, and $W_p = W_n = -0.09$. For the 1.88-MeV (0_2^+) state we used a monopole transition density of the form[21]

$$\rho_{\mathrm{tr},i}(r) = 3\rho_i(r) + r \frac{d\rho_i(r)}{dr} \quad (i = \mathrm{p,n}) , \tag{4}$$

In terms of the ground state density distribution parameters (R_i, a_i, and W_i), $\rho_{\mathrm{tr},i}(r)$ can be written explicitly as

$$\rho_{\mathrm{tr},i}(r) = \rho_0 \beta_i \left[\frac{(3 + 5 W_i x_i^2)}{1 + e^{[(r - R_i)/a_i]}} - \frac{\dfrac{r}{a_i}(1 + W_i x_i^2) e^{[(r - R_i)/a_i]}}{(1 + e^{[(r - R_i)/a_i]})^2} \right] \quad (i = \mathrm{p,n}) , \tag{5}$$

where $x_i = r/R_i$ and β_i is the (neutron or proton) monopole transition strength. The proton radius parameter R_p was adjusted to 4.41 fm for the monopole transition density in order to reproduce the experimental transition radius

$$R_{tr} = (\langle r^4 \rangle_{tr} / \langle r^2 \rangle_{tr})^{1/2} = 6.5 \pm 0.4 \text{ fm} \quad (6)$$

measured in an (e,e') experiment.[22] The neutron radius parameter was also increased by the same factor to 4.78 fm. Figure 2 shows the measured inelastic differential cross sections to the low-lying states in ^{44}Ca, together with the distorted-wave impulse-approximation (DWIA) calculations.

The data points for the 1.16-MeV (2_1^+) and 3.31-MeV (3_1^-) states include the previously reported cross sections[1,2] for these states at 180 MeV (crosses) and the cross sections from the present experiment (solid squares). These states, as well as the very weak 4_1^+ and 2_2^+ states at 2.28 and 2.66 MeV, are remarkably well fitted by the impulse-approximation calculations with collective-model transition densities. This success is apparently due to the fact that these excitations are characterized by surface-peaked transition densities and thus are not sensitive to the penetration of pion waves into the nuclear medium. The DWIA curve shown with the monopole transition to the 0_2^+ state at 1.88 MeV does not represent a fit to the data (since the data are rather structureless) but aimed only to check the agreement in magnitude between the data and DWIA calculations using information from (e,e'). In these calculations we constrained the deformation parameter (β_p) to give the value of $M_p = 5.45$ fm^2 from (e,e') (Refs. 22 and 30) and set arbitrarily $M_n = M_p$. This constraint yields $\beta_n = 0.087$ and $\beta_p = 0.114$. The calculated curves for π^+ and π^- agree quite well in magnitude without any normalization factor with the data points at forward angles, but the structure in the calculated curves is absent in the data—which exhibit a monotonic decrease with increasing angle. In this case the transition density has a volume distribution and thus is more sensitive to the penetration of the pion waves. This may indicate that the DWIA calculations do not describe pion distorted waves correctly in the nuclear interior as has been suggested in some previous pion inelastic studies.[23–27] The observed discrepancy for the monopole is discussed in more detail later in this communication.

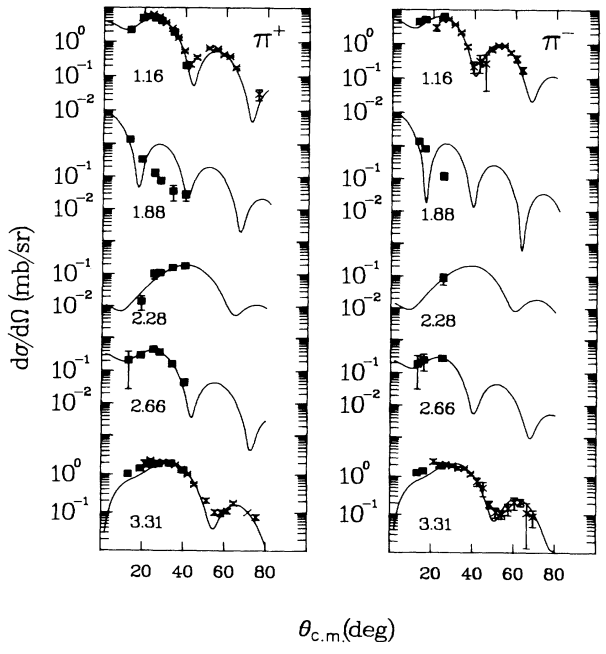

FIG. 2. Differential cross sections for π^+ and π^- inelastic scattering at 180 MeV for the low-lying states in ^{44}Ca (solid squares). Crosses represent cross sections measured at 180 MeV, from Refs. 1 and 2; solid lines are DWIA calculations with collective-model transition densities.

The matrix elements obtained from the impulse-approximation calculations described above are compared with those resulting from hadronic and electromagnetic measurements in Table I. There are two solutions for M_n and M_p, one with amplitudes in phase and the other with amplitudes out of phase, which give a simultaneous fit to π^+ and π^- inelastic scattering.[8,28] The first corresponds to predominantly an isoscalar transition and the second to an isovector transition. Since the low-lying transitions are expected to be predominantly isoscalar, the solution with M_n and M_p in phase is assumed. We also list in the table the ratios M_n/M_p and the isoscalar transition matrix elements M_0. There is excellent agreement between the present work and the electromagnetic data for the 2_1^+ state at 1.16 MeV. The electromagnetic values of M_p were extracted from values of $B(El)\downarrow$ using the relation

$$M_p = [B(El)(2J_i + 1)]^{1/2} , \quad (7)$$

where J_i is the angular momentum of the excited state. The deduced proton matrix element for the $l = 4$ transition to the 2.28-MeV state ($M_p = 197.6 \pm 17.8$ e fm^4) is in excellent agreement with the electron inelastic-scattering measurement of Ref. 33.

For the $E2$ and $E3$ transitions to the 2_2^+ and 3_1^- states at 2.66 and 3.31 MeV, respectively, only a lower limit on M_p can be calculated (Table I) from the electromagnetic data. The first has an electromagnetic value of M_p larger than that deduced from the pion data. However, a much smaller matrix element ($M_p = 3.4$ e fm^2) was listed in Ref. 34 for this transition with a nuclear deformation length of $\delta_N = 0.5$ fm. The second solution for M_n and M_p for the 2_2^+ state at 2.66 MeV gives $M_n = -11.9$ e fm^2 and $M_p = 13.9$ e fm^2. This solution is in better agreement with EM data ($M_p > 10.67$ e fm^2), but is in large disagreement with the isoscalar matrix elements deduced from the inelastic transition rate measured in the (α,α') work of de Voigt *et al.*[31] A more accurate lifetime measurement for this state would help to resolve this discrepancy. The $E3$ matrix element to the 3.31-MeV state ($M_p = 99.0 \pm 9.8$ e fm^3) is in agreement with the lower limit listed in Table I. The deduced isoscalar transition matrix elements from the present work are, in

TABLE I. Matrix elements in ^{44}Ca extracted from pion inelastic scattering compared with results from other nuclear probes.

			Present work				(α,α')	*EM*
E_x (MeV)	J^π	l	M_p (e fm^l)	M_n (e fm^l)	M_n/M_p	M_0 (e fm^l)	M_0[a] (e fm^l)	M_p (e fm^l)
1.16	2_1^+	2	20.7±1.86	28.4±2.5	1.37±0.16	24.6±1.55	22.5±3.4	21.3±0.7[b]
2.28	4_1^+	4	197.6±17.8	212.4±19.1	1.08±0.13	205±13.1	181.7±27.3	190.5±5.6[c]
2.66	2_2^+	2	7.4±0.7	5.1±0.46	0.69±0.08	6.25±0.34	8.3±1.3	> 10.67[d]
3.31[e]	3_1^-	3	99.0±9.8	105.4±10.4	1.06±0.13	102.2±7.1	90.9±13.6	> 73.9[d]

[a]Calculated from the isoscalar strengths measured in Ref. 31.
[b]Calculated from $B(El)\downarrow$ (Ref. 29) using the relation $M_p=[B(El)(2J_i+1)]^{1/2}$.
[c]References 33 and 34.
[d]Calculated from measured γ decay mean lifetime and branching ratio (Ref. 16). The uncertainty in M_p arises from the fact that only an upper limit on lifetime has been reported for this state, rather than from uncertainties in mixing or branching ratios.
[e]Doublet, 3.30 MeV (2^+) and 3.31 MeV (3^-).

most cases, in close agreement with the results from α inelastic scattering.[31]

Some features of the data can be qualitatively understood using a simple shell-model picture. The ratio M_n/M_p is 1.37±0.16 for the 2_1^+ state, but is only 1.06±0.13 for the 3^- state at 3.31 MeV. The 2_1^+ state in ^{44}Ca (as well as in other calcium isotopes with $N>20$) is mainly formed by neutron excitations, because $1\hbar\omega$ space proton excitations can contribute only to negative-parity states. On the other hand, the 3_1^- state can be excited either by proton or neutron excitations. Thus, for this state, M_n is approximately equal to M_p (or close to the hydrodynamical model prediction of $M_n/M_p=N/Z=1.2$). This effect has been observed even more clearly in ^{48}Ca, where the ratio M_n/M_p for the 2_1^+ state is more than twice as large as that for the 3_1^- state.[2] We note, however, that in both ^{44}Ca and ^{48}Ca nuclei the transition to the 2_1^+ state has clearly a collective nature, because a pure neutron-excitation should give a larger M_n/M_p ratio. This indicates the importance of core-excited pieces in the wave functions for these states. The pion data also indicate that the 2_2^+ state at 2.66 MeV has $M_p>M_n$ and therefore has an inverse character relative to the 2_1^+ state at 1.16 MeV.

Part of the disagreement in shape for the 0_2^+ state at 1.88 MeV may arise from a two-step reaction mechanism. Both this state and the ground state have a large $E2$ matrix element to the first excited 2_1^+ state at 1.16 MeV, with $B(E2;\ 0_2^+\rightarrow 2_1^+)=22\pm7$ W.u. and $B(E2;\ 2_1^+\rightarrow$ ground state$)=9.8\pm0.7$ W.u. Therefore, the 0_2^+ state could gain at least part of its strength from a transition through the 2_1^+ state at 1.16 MeV via the $0_1^+\leftrightarrow 2_1^+\leftrightarrow 0_2^+$ coupling. Previous studies of coupled-channel effects in pion scattering are limited.[23–27] In ^{12}C the coupled-channel impulse-approximation (CCIA) calculations, which included a complete $0_1^+\leftrightarrow 2_1^+\leftrightarrow 0_2^+$ coupling, significantly improved the fit to the monopole data at 50 and 162 MeV, Refs. 23 and 24, respectively. The CCIA calculations,[25] however, produced only very small changes for the inelastic scattering to the 2_1^+ state at 4.44 MeV in ^{12}C at $T_\pi=162$ MeV, although a larger effect was reported for this state at $T_\pi=100$ MeV.[27]

Static CCIA calculations have been performed using a three-parameter Fermi distribution for the ground-state density and a 25-MeV energy shift with the code CHOPIN.[32] In all CCIA calculations the proton transition densities were chosen to give the known $B(E2)$ value for each channel.[16,29] Figure 3 shows the $B(E2)$ values used in the calculations. The neutron transition density for the first step, ground state $\leftrightarrow 2_1^+$ (channel $1\leftrightarrow 2$) was taken to be identical to that obtained from the DWIA calculations (listed in Table I). For the second step (channel $2\leftrightarrow 3$), M_n was arbitrarily set equal to M_p. Here, channel 3 can be either the 0_2^+, 4_1^+, or 2_2^+ states shown in Fig. 3. The direct transitions were calculated using the known values of M_p from *EM* data listed in Table I. Except for the 0_2^+ states, the magnitude of M_n in the direct transition as well as the phases of M_n and M_p in the second step were varied to fit the data. For the ground state $\rightarrow 0_2^+$ direct transition we used the same monopole calculations as mentioned earlier. For the $\Delta J=2$ second step we used $M_p=14.2$ e fm^2 from

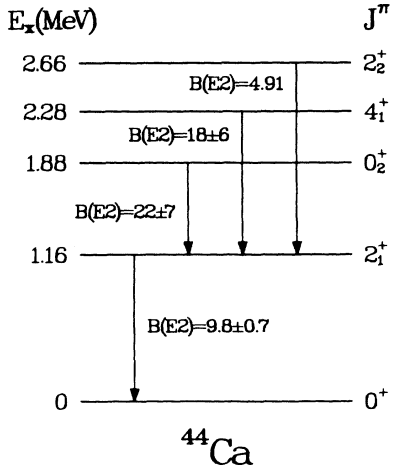

FIG. 3. $B(E2)$ values in Weisskopf units for transitions in ^{44}Ca used in the two-step coupled-channel impulse-approximation calculations.

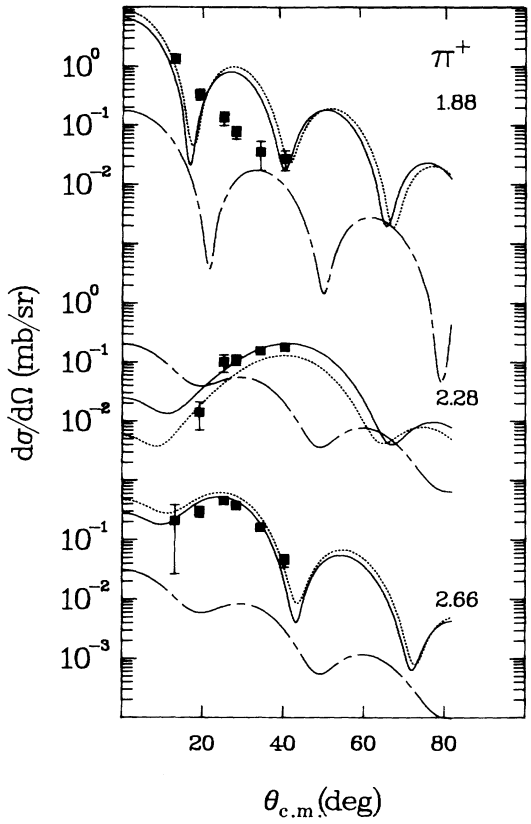

FIG. 4. Differential cross sections for π^+ inelastic scattering at 180 MeV compared with two-step static CCIA calculations (chain-dashed lines), direct one-step calculations (dotted lines), and full coupling calculations (solid lines). The calculations are explained in the text.

(e,e′) data and set $M_n = M_p$. The only parameters varied in this case were the signs of M_n and M_p in the second step.

Figure 4 shows again the angular distribution for the three weak transitions leading to the 0_2^+, 4_1^+, and 2_2^+ states in ^{44}Ca together with the CCIA calculations. The direct transitions (dotted lines) have been normalized as described earlier. The chain-dashed lines represent the contribution to pion inelastic scattering from two-step calculations with $0_1^+ \leftrightarrow 2_1^+ \leftrightarrow 0_2^+$, $0_1^+ \leftrightarrow 2_1^+ \leftrightarrow 4_1^+$, and $0_1^+ \leftrightarrow 2_1^+ \leftrightarrow 2_2^+$ couplings. The solid lines in the figure represent the full coupling calculations. Table II shows the neutron and proton multiple matrix elements used in the CCIA calculations for the 0_2^+ at 1.88 MeV. The calculations indicate that the two-step sequential cross section is quite small relative to the direct one-step cross section for the 0_2^+ state at 1.88 MeV, as well as for the 2_2^+ state at 2.66 MeV at $T_\pi = 180$ MeV, but that it is more significant for the $l = 4$ transition to the 2.28-MeV state. The full coupling curves shown in Fig. 4 have been calculated assuming both M_n and M_p have positive signs in all channel couplings, except for the 2.28-MeV (4_1^+) state where M_p in channel $2 \leftrightarrow 3$ coupling has a negative sign to give a better fit to our data and to the isoscalar matrix element M_0 measured in the (α,α') work.[31] The deduced neutron matrix elements for the direct transitions obtained by fitting the full-coupling curves to the data are 118.6 e fm^4 and 2.0 e fm^2 for the 2.28- and 2.66-MeV states respectively. If two-step contributions do exist in pion inelastic scattering then values of M_n obtained from DWIA analysis (Table I) may vary significantly due to the coupling of two-step and direct contributions. However, our data are inconclusive as to the existence of coupled-channel effects because they do not improve the fit for the monopole or the 2.28-MeV (4_1^+) and 2.66-MeV (2_2^+) states. Calculation assuming that $M_n = 0.73\ M_p$ (not shown in Fig. 4) for channel $2 \leftrightarrow 3$ coupling, i.e., the inverse ratio in the first step, obviously produce smaller changes.

TABLE II. The neutron and proton multipole matrix elements used in the coupled channel calculations for the 0_2^+ at 1.88 MeV.

Channel coupling $J_i^\pi \leftrightarrow J_f^\pi$	M_n (e fm^l)	M_p (e fm^l)
$0^+_{g.s.} \leftrightarrow 2_1^+$	28.4	20.7
$2_1^+ \leftrightarrow 0_2^+$	±14.2	±14.2
$0^+_{g.s.} \leftrightarrow 0_2^+$	5.45[a]	5.45[a]

[a]The monopole matrix element is defined in units of fm^2.

In summary, neutron and proton multipole-matrix elements for transitions to low-lying states in ^{44}Ca have been extracted from simultaneous fits to π^+ and π^- data at $T_\pi = 180$ MeV. The extracted values for M_n and M_p are in good agreement with electromagnetic data and isoscalar strengths measured in α inelastic scattering. DWIA calculations with collective-model transition densities give a good account for all transitions with $l > 0$. A discrepancy between DWIA calculations and the data was observed for the monopole transition to the 0_2^+ state at 1.88 MeV. We find no conclusive evidence as to the existence of two-step pion-scattering contributions for the weak low-lying triplet (0_2^+, 4_1^+, and 2_2^+) at 1.88, 2.28, and 2.66 MeV, respectively.

This work was supported in part by the U.S. Department of Energy, the Robert A. Welch Foundation, and the National Science Foundation. We wish to thank Allen Williams, Joseph McDonald, and Juan Garza for their help in data analysis, and Stephen F. Elston for his help in taking the data.

*Present address: Fermi Laboratory, Batavia, IL 60510.
†Present address: Los Alamos National Laboratory, Los Alamos, NM 87545.
‡Present address: Lawrence Berkeley Laboratory, Berkeley, CA 94720.
§Present address: Indiana University Cyclotron Facility, Bloomington, IN 47405.

[1]Kenneth G. Boyer *et al.*, Phys. Rev. C **24**, 598 (1981).
[2]K. G. Boyer *et al.*, Phys. Rev. C **29**, 182 (1984).
[3]H. T. Fortune and A. E. L. Dieperink, Phys. Rev. C **19**, 1112

(1979).
[4]W. J. Gerace and A. M. Green, Nucl. Phys. **A93**, 110 (1967); **A113**, 641 (1968); **A123**, 241 (1969).
[5]C. L. Morris *et al.*, Phys. Rev. C **24**, 231 (1981).
[6]C. Olmer *et al.*, Phys. Rev. C **21**, 254 (1980).
[7]S. J. Seestrom-Morris *et al.*, Phys. Rev. C **28**, 1301 (1983).
[8]C. L. Morris *et al.*, Phys. Rev. C **35**, 1388 (1987).
[9]C. L. Morris *et al.*, Phys. Rev. C **13**, 1755 (1976).
[10]S. J. Seestrom-Morris *et al.*, Phys. Rev. C **26**, 594 (1982).
[11]D. B. Holtkamp *et al.*, Phys. Rev. C **31**, 957 (1985).
[12]S. J. Seestrom-Morris *et al.*, Phys. Rev. C **31**, 923 (1985).
[13]C. L. Morris *et al.*, Nucl. Instrum. Methods A **238**, 94 (1985).
[14]G. Rowe, M. Salomon, and R. H. Landau, Phys. Rev. C **18**, 584 (1978).
[15]C. L. Morris (unpublished).
[16]P. M. Endt and C. Van der Leun, Nucl. Phys. **A310** (1978).
[17]R. A. Eisenstein and G. A. Miller, Comput. Phys. Commun. **11**, 95 (1976).
[18]F. James and M. Roos, Comput. Phys. Commun. **10**, 343 (1975).
[19]L. S. Kisslinger, Phys. Rev. **98**, 761 (1955).
[20]W. B. Cottingame and D. B. Holtkamp, Phys. Rev. Lett. **45**, 1828 (1980).
[21]N. Auerbach, Phys. Lett. **36B**, 293 (2171).
[22]H. D. Gräf *et al.*, Nucl. Phys. **A295**, 319 (1978).
[23]D. A. Sparrow and W. J. Gerace, Phys. Rev. Lett. **41**, 1101 (1978).
[24]C. L. Morris *et al.*, Phys. Rev. C **28**, 2165 (1983).
[25]C. L. Morris *et al.*, Phys. Rev. C **30**, 662 (1984).
[26]M. Gmitro, J. Kvasil, and R. Mach, Phys. Lett. **113B**, 205 (1982).
[27]C. Steven Whisnant, Phys. Rev. C **33**, 1443 (1986).
[28]S. Mordechai *et al.*, Phys. Rev. C **36**, 710 (1987).
[29]P. M. Endt, At. Data Nucl. Data Tables **23**, 3 (1979).
[30]M. Ulrickson *et al.*, Phys. Rev. C **15**, 186 (1977).
[31]M. J. A. de Voigt, D. Cline, and R. N. Horoshko, Phys. Rev. C **10**, 1798 (1974).
[32]E. Rost, computer code CHOPIN (unpublished).
[33]J. Heisenberg, J. S. McCarthy, and I. Sick, Nucl. Phys. **A164**, 353 (1971).
[34]K. E. Rehm *et al.*, Phys. Rev. C **25**, 1915 (1982).